Table S1. Information and properties from each of the columns tested in this analysis.

Column	Column manufacturer, part number, and parameters	Stationary phase properties
C18	ACQUITY UPLC® BEH C18, 186002350, 130 Å pore size, 1.7 µm particles, 2.1×50 mm	Trifunctionally bonded BEH phase that is stable from pH 1-12. Traditional nonpolar interactions.
HILIC	CORTECS™ UPLC® HILIC, 186007104, 90 Å pore size, 1.6 µm particles, 2.1×50 mm	Stable from pH 1 to 5, intended for extremely polar compounds. Unbonded stationary phase
Amide	ACQUITY UPLC® BEH Amide, 186004800, 130 Å pore size, 1.7 µm particles, 2.1×50 mm	Trifunctionally bonded amide phase that is stable from pH 2 to 12. Intended for compounds with a wide range of polarities, including those that are too polar for many RPLC columns
2-EP	Viridis UPC^2™ BEH 2-Ethylpyridine, 186006578, 130 Å pore size, 1.7 µm particles, 2.1 mm×100 mm	Designed for good retention without the use of additives, less polar than the similar BEH column.
BEH	Viridis UPC^2™ BEH, 186006564, 130 Å pore size, 1.7 µm particles, 3.0×100 mm	Ethylene bridged hybrid particles for interaction with polar functional groups.

Table S2. Masses observed in this study, along with previously reported proposed chemical structures. Retention times given are for peaks observed using the BEH column with pure methanol as the mobile phase modifier. Retention times shown in bold indicate most intense signals. Fragments are given for those peaks that show significant fragmentation.

m/z	Neutral chemical formula	Proposed neutral structure	Retention time (min)	Fragment *m/z*	Reference
59			4.5, **6.9**, 15	42	This study
81			6.9	No significant fragments	This study
83	$C_4H_7N_2$	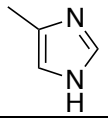	5.5, **12.8**, 14.8	5.5 and 12.8: 41, 56	(Kampf et al., 2016)
87			1.2, **2.8**, **4.5**, 15.6	2.8 and 4.5: 43, 45, 59	This study
97	$C_5H_8N_2$	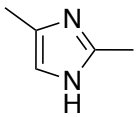	5.2, 8.3, **14.3**	8.3: 42, 69 14.3: 42, 56	(De Haan et al., 2011; Hawkins et al., 2018)
98			**2.0**, 3.9, 5.0	2.0: 43, 56, 70	This study
109	$C_6H_8N_2$	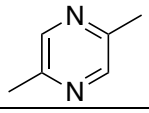	3.7	41, 55, 68, 82, 93	(Lin et al., 2015; Hawkins et al., 2018)
113			3.9	95, 85, 67, 45, 43	This study
117			**2.7**, 4.3, 4.9, 5.8	2.7: 45, 59, 87 4.3: 43, 57, 85 4.9: 43, 71, 99 5.8: 41, 59	This study
122			**3.9**, 14.7	56, 104	This study
125	$C_6H_8ON_2$	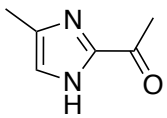	5.5	43, 56, 83, 107	(De Haan et al., 2011; Kampf et al., 2012; Lin et al., 2015; Hawkins et al., 2018)
126	$C_6H_7O_2N$	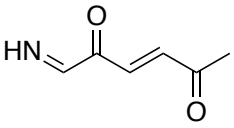	2.2, 3.6, 4.1, 5.0, **13.4**, **14.9**	2.2: 43, 84, 111 13.4 and 14.9: 42, 55, 70, 80, 98, 108	(Sareen et al., 2010; Lin et al., 2015)
127			2.2, **5.8**, 8.2	5.8: 83 8.2: 89, 56	This study
131			**1.7**, **3.8**, 4.6	1.7: 45, 59, 73 3.8: 43, 45, 67, 85, 113 4.6: 45, 59, 87	This study

m/z	Neutral chemical formula	Proposed neutral structure	Retention time (min)	Fragment *m/z*	Reference
139			5.2, 5.3, 5.8, 5.9, 6.7, **11.4**, **12.3**	5.2: 97 5.3: 57, 83 12.3: 57, 83, 96, 139	This study
144	$C_6H_9O_3N$	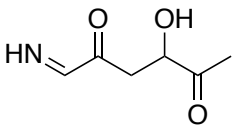	**2.3**, 3.9, 4.2, 8.3, 8.6	3.9: 56, 74 4.2: 102, 126 8.3: 60, 74, 102 8.6: 74	(Sareen et al., 2010; Lin et al., 2015)
162	$C_9H_{11}N_3$ $C_6H_{11}O_4N$	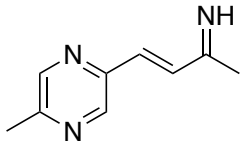 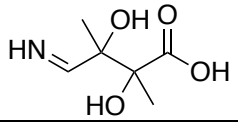	**7.7**, 7.9, 15.6	7.7: 42, 66, 80, 94, 107, 121, 135, 147 15.6: 42, 88	(Lin et al., 2015; Hawkins et al., 2018) (Sareen et al., 2010; Lin et al., 2015)
165	$C_9H_{12}ON_2$		4.8, 6.1, **6.7**	6.1 and 6.7: 43, 123, 147	(Lin et al., 2015)
166	$C_9H_{11}O_2N$		**4.0**, 4.5, 7.4, 9.3, 10.0	4.0: 42, 79, 124, 148 9.3: 96, 110, 138	(Lin et al., 2015)
167	$C_9H_{10}O_3$		**1.8**, 2.1, 2.5, 4.3, 5.9, 6.1, 7.3, 10.3, 11	1.8: 43, 79, 93, 107, 125, 149 7.3: 43, 97	(Lin et al., 2015)
169			1.3, **4.3**, **4.6**, **4.8**, 4.7, 6.1, **7.6**, 8.3, 14.7	4.3: 43, 53, 109, 151 4.4: 59, 71, 83, 111, 127	This study
178	$C_9H_{11}N_3O$	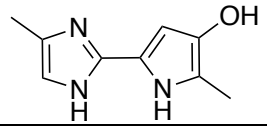	1.9, 6.9, 7.2, **8.3**, 9.3, 9.8, 9.9	6.9: 82, 114 9.8: 148	(Aiona et al., 2017)
180	$C_9H_9NO_3$	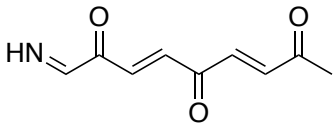	3.2, 3.8, 4.0, **8.3**	3.8: 45, 57, 89, 101, 107 8.3: 84, 98, 110	(Lin et al., 2015; Hawkins et al., 2018)
181	$C_9H_{12}N_2O_2$	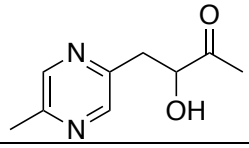	4.5, 5.5, **5.8**, 7.3, 9.3, 9.5	5.8: 139 7.3: 83, 99, 121	(Hawkins et al., 2018)

m/z	Neutral chemical formula	Proposed neutral structure	Retention time (min)	Fragment *m/z*	Reference
183	$C_9H_{14}O_2N_2$		**4.2**, **6.8**, 9.2, **9.5**, 13.4	4.2: 109, 151 9.2: 141 9.5: 112 13.4: 110, 123	(Lin et al., 2015)
190			1.8, **4.8**, 5.0, **5.3**, **5.4**, 5.6	4.8: 106, 150, 162 5.0: 69, 148 5.3: 94, 106, 150, 162 5.4: 83, 109, 148, 163, 172	This study
195	$C_9H_{10}N_2O_3$	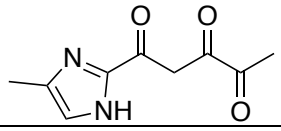	5.0, **5.3**, 5.6	5.3: 98, 139	(Aiona et al., 2017)
196	$C_9H_{13}O_2N_3$	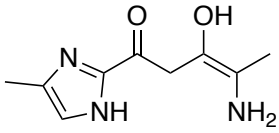	7.6, **7.8**, 9.8, 10.8, 14.7	7.6: 43, 126, 178 7.8: 67, 79, 84, 95, 122, 136, 164 9.8: 95, 138, 168 10.8: 83, 137, 154 14.7: 150, 178	(Sareen et al., 2010; Lin et al., 2015)
197	$C_9H_{12}O_3N_2$	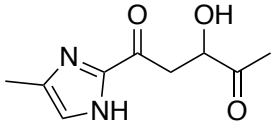	1.2, 7.7, 7.8, **8.7**	1.2: 95 7.8: 123, 137, 151, 179 8.7: 83, 97, 109, 125, 151, 161, 179	(Sareen et al., 2010; Lin et al., 2015)
216	$C_9H_{13}NO_5$	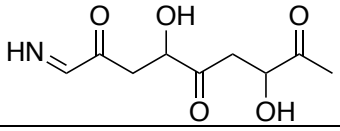	4.6, 7.9, 8.0, **9.5**	7.9 and 9.5: 174, 188	(Hawkins et al., 2018)
224			**2.8**, 6.3, 6.7, 7.2, 8.3, **8.4**, 10.6	2.8: 59, 73, 87, 103, 117, 189 6.7: 43, 122, 140, 154, 164, 182, 206 7.2: 182, 194	This study
232	$C_{12}H_{13}O_2N_3$	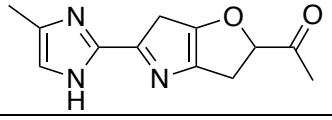	7.8, 8.6, **9.3**, 10.1, 10.4, 10.8	7.8: 162 9.3: 43, 83, 192, 204	(Lin et al., 2015; Aiona et al., 2017)

m/z	Neutral chemical formula	Proposed neutral structure	Retention time (min)	Fragment *m/z*	Reference
234	$C_{12}H_{11}NO_4$	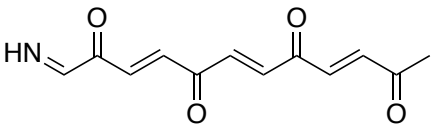	3.6, 7.9, 8.6, **8.9**, 10.2, 10.4, 10.8, 10.9, 11.1, 16.5	7.9: 109, 110, 151, 192 8.9: 162, 188, 216 10.8: 216 16.5: 188	(Hawkins et al., 2018)
235	$C_{12}H_{14}N_2O_3$	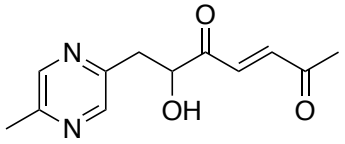 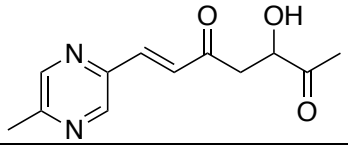	8.7	83, 108, 217	(Hawkins et al., 2018)
250	$C_{12}H_{16}O_3N_3$	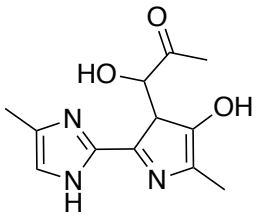	10.1, 10.4, 10.8	All peaks: 190, 208, 232	(Amarnath et al., 1994; Bones et al., 2010; Lin et al., 2015)
251	$C_{12}H_{14}O_4N_2$	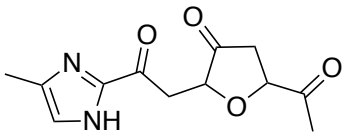 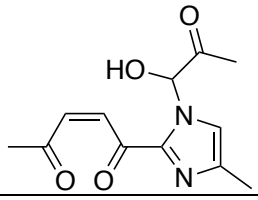	**7.4**, 8.8, 9.2, 15.2	7.4: 167, 191, 209, 233, 251	(Sareen et al., 2010; Kampf et al., 2012; Lin et al., 2015)
253			8.2, **8.4**, 8.9, 9.4	8.4: 83, 87, 123, 139, 150, 193, 235 9.4: 125, 193, 235	This study
269	$C_{12}H_{16}O_5N_2$	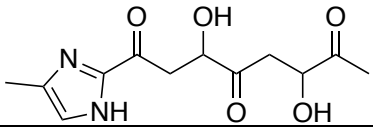	**1.9**, 11.1	11.1: 83, 125, 227	(Lin et al., 2015; Aiona et al., 2017)
288	$C_{12}H_{17}NO_7$	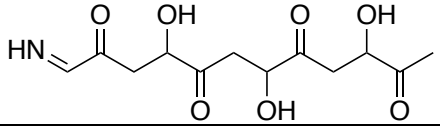	**7.9**, 9.4, **10.0**, 10.6	No significant fragments	(Hawkins et al., 2018)
289	$C_{15}H_{16}N_2O_4$	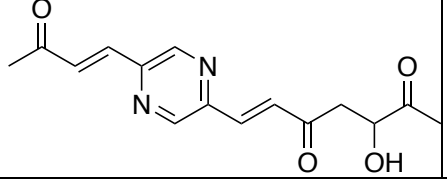	4.5, 10.0	No significant fragments	(Hawkins et al., 2018)

m/z	Neutral chemical formula	Proposed neutral structure	Retention time (min)	Fragment *m/z*	Reference
306	$C_{15}H_{19}O_4N_3$	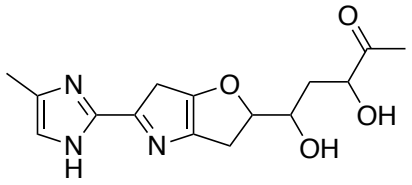	5.1, 9.3, 9.65, 9.73, **10.1**, **10.2**, 10.6	9.3: 234 9.65, 10.1, and 10.2: 192, 234 9.73 and 10.6: 246, 288	(Lin et al., 2015; Aiona et al., 2017)
323	$C_{15}H_{18}N_2O_6$	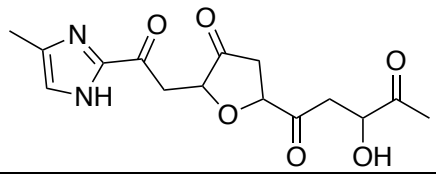	7.4, **10.0**	No significant fragments	(Lin et al., 2015; Aiona et al., 2017)

Mass spectrometry parameters

Performing a scan over the entire mass region of interest supplies necessary information about the analytes present, but for improved sensitivity and signal to noise ratios, extracted ion chromatograms (EICs) were utilized extensively. Full spectral scans from *m/z* 50-350 were used to identify possible products of interest, then subsequent samples monitored each of the identified masses. This process was repeated until as many features as possible were maintained to ensure that all compounds were accounted for. A comparison between a scan and the combined EIC data are shown in Fig. S2. All masses observed in this study are given in Table S2 and all EICs are shown in Fig. S3. Full spectral scans were also taken for each separation to ensure no new compounds were missed during analysis. All other chromatograms presented in this study are a combination of all the EIC signals in Table S2 and Fig. S3.

For EIC collection, a mass window of ±0.5 Da from the desired mass is monitored. Therefore, it is possible to falsely identify masses within the system that are not real if an adjacent mass has a very high intensity. One example of this can be seen with the peak from *m/z* 97 and 98 that elutes at 14.3 min in Fig. S3. This peak is very intense at *m/z* 97 and shows up in *m/z* 98 at ~10× lower intensity. This peak can also be seen at this lower intensity at *m/z* 96 (not shown), indicating that this is likely a result of the fact that a quadrupole mass spectrometer only has unit resolution and cannot easily distinguish between adjacent masses. It is possible to determine if a mass is found in a reaction mixture by analyzing masses within 1 Da of the mass of interest. This was done here in order to ensure that all masses reported in Table S2 are not artifacts of the mass selector used.

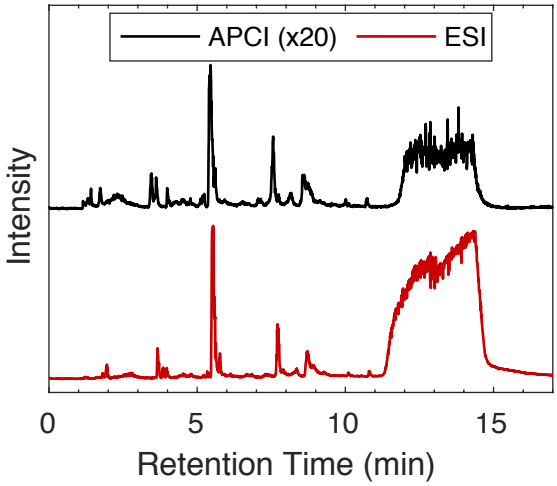

Figure S1. Electrospray ionization (ESI, red) and atmospheric pressure chemical ionization (APCI, black) combined extracted ion chromatograms. The APCI signal is multiplied by 20 for comparison with the ESI signal. Both ionization methods detected most peaks, but all peaks were detected by ESI and with significantly higher signal.

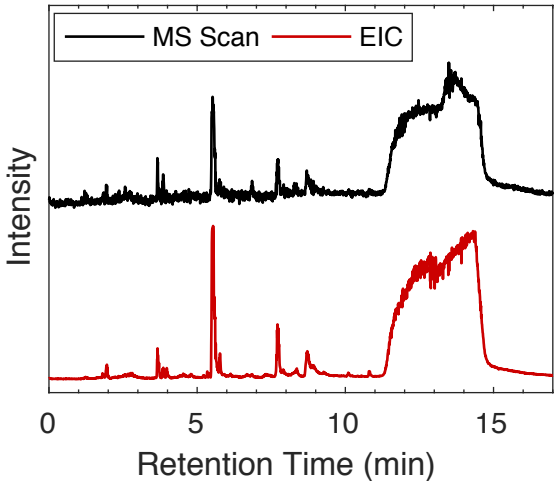

Figure S2. Comparison of the total MS scan (black) with the combined extracted ion chromatograms (EIC, red) of all masses monitored. The noise is significantly decreased in the EIC scan but most spectral features are maintained.

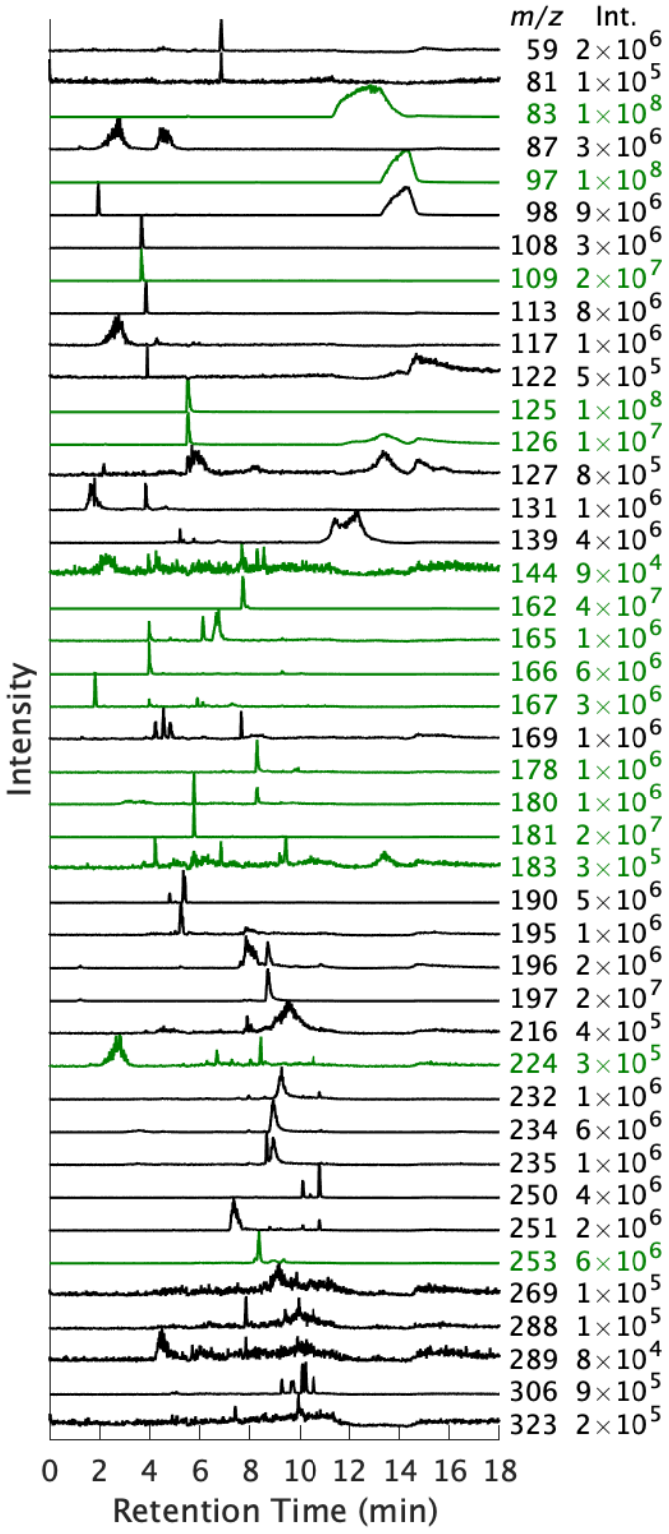

Figure S3: Extracted ion chromatograms of all m/z values seen under the conditions described above. All chromatograms have been normalized to their maximum value for ease of viewing due to the very intense signals given by imidazole derivatives. The intensity of the largest peak is given to the right of each trace. The traces shown in green correspond to masses that have been observed in previous work and those shown in black have not yet been published for this system (Lin et al., 2015; Hawkins et al., 2018).

REFERENCES

Aiona, P. K., Lee, H. J., Leslie, R., Lin, P., Laskin, A., Laskin, J., and Nizkorodov, S. A.: Photochemistry of Products of the Aqueous Reaction of Methylglyoxal with Ammonium Sulfate, ACS Earth Space Chem., 1, 522-532, 10.1021/acsearthspacechem.7b00075, 2017.

Amarnath, V., Valentine, W. M., Amarnath, K., Eng, M. A., and Graham, D. G.: The mechanism of nucleophilic substitution of alkylpyrroles in the presence of oxygen, Chem. Res. Toxicol., 7, 56-61, 10.1021/tx00037a008, 1994.

Bones, D. L., Henricksen, D. K., Mang, S. A., Gonsior, M., Bateman, A. P., Nguyen, T. B., Cooper, W. J., and Nizkorodov, S. A.: Appearance of strong absorbers and fluorophores in limonene-O_3 secondary organic aerosol due to NH_4^+-mediated chemical aging over long time scales, J. Geophys. Res.: Atmos., 115, D05203, 10.1029/2009JD012864, 2010.

De Haan, D. O., Hawkins, L. N., Kononenko, J. A., Turley, J. J., Corrigan, A. L., Tolbert, M. A., and Jimenez, J. L.: Formation of Nitrogen-Containing Oligomers by Methylglyoxal and Amines in Simulated Evaporating Cloud Droplets, Environ. Sci. Technol., 45, 984-991, 10.1021/es102933x, 2011.

Hawkins, L. N., Welsh, H. G., and Alexander, M. V.: Evidence for pyrazine-based chromophores in cloud water mimics containing methylglyoxal and ammonium sulfate, Atmos. Chem. Phys., 18, 12413-12431, 10.5194/acp-18-12413-2018, 2018.

Kampf, C. J., Jakob, R., and Hoffmann, T.: Identification and characterization of aging products in the glyoxal/ammonium sulfate system -- implications for light-absorbing material in atmospheric aerosols, Atmos. Chem. Phys., 12, 6323-6333, 10.5194/acp-12-6323-2012, 2012.

Kampf, C. J., Filippi, A., Zuth, C., Hoffmann, T., and Opatz, T.: Secondary brown carbon formation via the dicarbonyl imine pathway: nitrogen heterocycle formation and synergistic effects, Phys. Chem. Chem. Phys., 18, 18353-18364, 10.1039/C6CP03029G, 2016.

Lin, P., Laskin, J., Nizkorodov, S. A., and Laskin, A.: Revealing Brown Carbon Chromophores Produced in Reactions of Methylglyoxal with Ammonium Sulfate, Environ. Sci. Technol., 49, 14257-14266, 10.1021/acs.est.5b03608, 2015.

Sareen, N., Schwier, A. N., Shapiro, E. L., Mitroo, D., and McNeill, V. F.: Secondary organic material formed by methylglyoxal in aqueous aerosol mimics, Atmos. Chem. Phys., 10, 997-1016, 10.5194/acp-10-997-2010, 2010.